Statistical nature of nuclear multifragmentation

R. Donangelo and S. R. Souza
Instituto de Física, Universidade Federal do Rio de Janeiro, C.P. 68528, 21945-970 Rio de Janeiro, Brazil
(Received 8 November 1996)

A recent analysis of multifragmentation data in terms of an elementary binary decay appears to imply that the decay is sequential and from a thermalized source. This last feature would imply a lack of sensitivity to dynamical effects, at least in this multifragmentation data. We discuss this analysis using a simultaneous statistical multifragmentation model (SMM), which assumes decay from a thermalized source, and also employing a molecular dynamics model (MDM). The elementary binary decay analysis of the SMM predictions yields results which are qualitatively similar to those of the data. The differences are shown to stem from superposition of processes associated with very different impact parameters. Thus the data are not inconsistent with simultaneous decay. The MDM calculations, on the other hand, disagree with the data. We suggest, however, that more reliable dynamical calculations are needed before accepting an absence of dynamical effects in these data. [S0556-2813(97)04608-6]

PACS number(s): 25.70.Pq, 24.60.Dr

I. INTRODUCTION

The possibility of a liquid-gas phase transition in nuclear matter [1–8], based on the fact that its thermal equilibrium phase diagram is quite similar to that of a van der Waals system, has instigated intensive experimental [9–15] and theoretical [16–25] investigations in proton-induced reactions at a few GeV's and in heavy-ion reactions at energies ranging from a few tens to a few hundreds of MeV per nucleon. Such studies revealed that the breakup of nuclear systems into complex fragments ($Z \geqslant 3$), also called intermediate mass fragments (IMF's), is the most important reaction mechanism in central and midcentral heavy-ion collisions in the energy domain mentioned above (see [26] for a recent review on the subject). In spite of large theoretical and experimental efforts, the actual mechanisms which cause nuclei to break up into these sizable fragments could not be completely elucidated yet. As a matter of fact, it has been only very recently that a few experimental indications concerning this liquid-gas phase transition have been found [27].

In this context, considerations based on an appreciable amount of experimental data indicate that the mechanisms responsible for the breakup of nuclear matter into IMF's are of a statistical nature [28–31]. More precisely, experimental analyses clearly suggest that the relative IMF multiplicities depend only on the excitation energy of the system, being independent of the colliding nuclei and bombarding energy [28]. Furthermore, these experimental results suggest that the multifragment emission can be reduced to elementary binary emission [29,31] and that its thermal properties are not sensitive to the entrance channel [31].

In this work, we investigate the extent to which the statistical nature of the IMF emission can be inferred from the analyses mentioned above. We examine these aspects by means of two different approaches: the Copenhagen statistical multifragmentation model (SMM) [21] and the molecular dynamics model (MDM) [25,32]. The SMM assumes that fragments are created due to the prompt breakup of a source in thermal equilibrium. On the other hand, in the MDM, the evolution drives the system to configurations in which dynamic instabilities grow, leading to its breakup.

Since these models are based on quite distinct scenarios for the dissociation, one may thus ascertain whether any of them are compatible with the experimental observations [29–31]. This may give us further insight into the underlying physics of the multifragmentation process.

The paper is organized as follows: in Sec. II we briefly recall the main features of the models we use. Results and discussion are presented in Sec. III. Concluding remarks are drawn in Sec. IV.

II. MODELS

In this section we outline the most important physical aspects of the models employed in this work, which are discussed in detail in Refs. [21] and [32].

A. Copenhagen statistical multifragmentation model

The SMM assumes that, as a consequence of the nuclear collision, a hot and expanded composite system is formed and, most important for our discussion, that the system is in thermodynamic equilibrium when it reaches its breakup configuration. The dissociating hot nuclear system is thus characterized, within this model, solely by its mass and atomic numbers, excitation energy, and volume.

In order to study the breakup of the system, the model considers that the relative statistical weight of a fragmentation mode $\{f\}$ is

$$\Gamma(\{f\}) = \exp S(\{f\}), \tag{2.1}$$

where $S(\{f\})$ is the entropy of the system in this particular breakup configuration. The entropy $S(\{f\})$ contains contributions from the thermal motion of the fragments inside the breakup volume, as well as from their internal excitation. The latter are obtained from an extension of the liquid drop model to hot nuclear matter.

The average value of a physical quantity Q is then obtained as

 © 1997 The American Physical Society

$$\langle Q\rangle = \frac{\Sigma_{\{f\}} Q(\{f\})\Gamma(\{f\})}{\Sigma_{\{f\}}\Gamma(\{f\})}, \tag{2.2}$$

where $Q(\{f\})$ is the value of the physical quantity for the fragmentation mode $\{f\}$, and the sum is over all possible modes satisfying mass, charge, and energy conservation.

The direct evaluation of the sum in Eq. (2.2) is almost impossible for a large system, due to the huge number of different fragmentation modes. This number is even much greater than in the original version of the SMM [21] because now the isospin degrees of freedom have been included into the model [33]. Therefore one resorts to the Monte Carlo method in order to evaluate this sum.

It is important to remark that the SMM assumes that all fragments are formed at the same time. Thus the decay is assumed to be not only statistical from a thermally equilibrized system, but also simultaneous. In order to preserve this last characteristic, in the calculations presented in this work we do not include the binary decay of the hot primary fragments. This is consistent with the MD calculations to be presented below, since it is not possible for them to consider the evolution of the system for the time needed for the primary fragments to cool down.

B. Molecular dynamics model

In the molecular dynamics approach the time evolution of the position $\mathbf{r}_i$ and momentum $\mathbf{p}_i$ of the ith nucleon is dictated by classical equations of motion [32]

$$\frac{d\mathbf{r}_i}{dt} = \frac{\partial \mathcal{H}}{\partial \mathbf{p}_i} \tag{2.3}$$

and

$$\frac{d\mathbf{p}_i}{dt} = -\frac{\partial \mathcal{H}}{\partial \mathbf{r}_i} + \mathbf{C}_i(t). \tag{2.4}$$

The Hamiltonian of the system, $\mathcal{H}$, has contributions from the kinetic energy and the Coulomb repulsion between protons, besides terms associated with a Skyrme-type and a Yukawa-type isospin-dependent effective interaction [32]. Effects associated with hard collisions between nucleons are introduced phenomenologically into the model by means of the collision term $\mathbf{C}_i(t)$. More precisely, whenever two nucleons get closer than $\sqrt{\sigma/\pi}$, where σ represents the nucleon-nucleon cross section, the model considers that they collide. Their momenta are then randomly changed, but in such a way that energy and momentum are conserved in each collision. Since nucleons are fermions, effects associated with the Pauli principle are phenomenologically incorporated by allowing collisions only if the phase space region corresponding to the final state of the nucleons is available.

The initial configuration of the system is carefully chosen so as to reproduce the gross properties of finite nuclei. Here we give a brief description of the procedure we adopt. A detailed discussion may be found in Ref. [32]. The positions of the nucleons are homogeneously sampled within a sphere of radius $1.14A^{1/3}$ fm, where A stands for the mass number of the nucleus. The neutron and proton densities are calculated and then the Fermi momentum $p_F(\mathbf{r})$, at any point of the sphere, is obtained in the local-density approximation. The momentum $\mathbf{p}_i$ of the ith nucleon is drawn in a sphere of radius $p_F(\mathbf{r}_i)$. The momentum $\mathbf{p}_i$ is accepted if the binding energy of the nucleon is larger than 6.5 MeV and if the phase space region into which the nucleon would be placed is available. The final configuration of the system is accepted if the binding energy of the nucleus lies between 8.0 and 9.0 MeV per nucleon. Since the procedure briefly described above does not ensure that the nuclei are generated in a stationary state, an isolated ''ground-state'' nucleus should emit a few nucleons after a while. We have checked that nuclei generated in this way remain fairly stable within 200 fm/c. More precisely, no nucleons are emited before 100 fm/c and only 1% of the nucleons escapes until 200 fm/c (see Ref. [32]).

Nucleus-nucleus collisions are simulated by boosting two nuclei against one another with appropriate values of kinetic energy and impact parameter. The dynamic evolution of the system is followed until 200 fm/c. At this moment, a cluster analysis is performed so as to identify the fragments produced in the collision. We have adopted the criterion used in Refs. [34,35] for defining clusters; i.e., two nucleons are assumed to be linked together if the distance between them is smaller than 3 fm.

It is important to realize that, in the framework of this model, fragments are formed due to dynamic instabilities which grow naturally during the dynamic evolution of the system.

III. RESULTS AND DISCUSSION

The models considered in this work are able to predict fragment distributions such as those discussed in Refs. [29–31]. In this section we apply them to examine the qualitative features of multifragment emission. We stress, however, that our calculations are not intended to adjust any details of the experimental data, but just to understand the main properties of those models. In particular, while the SMM model has as an input the excitation energy of the hot nuclear system, the MDM calculations and the data give the results in terms of the transverse energy. It is precisely from the comparison between the fragment production in terms of these two quantities that we extract important consequences on their connections, as we will see below.

A. Predictions of the SMM

We consider a nuclear system similar to the hot region formed in the $^{36}\mathrm{Ar}+^{197}\mathrm{Au}$ collisions studied in the experimental work of Ref. [29]. We take the mass and atomic numbers to be $A=160$ and $Z=60$, respectively, and the excitation energy ranging from 1 to 8 MeV per nucleon. The breakup density of this source is assumed to be $\rho=0.05$ nucleons/fm^3.

The solid triangles in Fig. 1 show the mean IMF multiplicity as a function of the excitation energy corresponding to the simultaneous statistical breakup of the source just described. The figure shows that the average IMF multiplicity rises from zero, at low excitation energies, to values larger than 10 at the highest excitation energies considered here. This behavior should be expected since, as mentioned above,

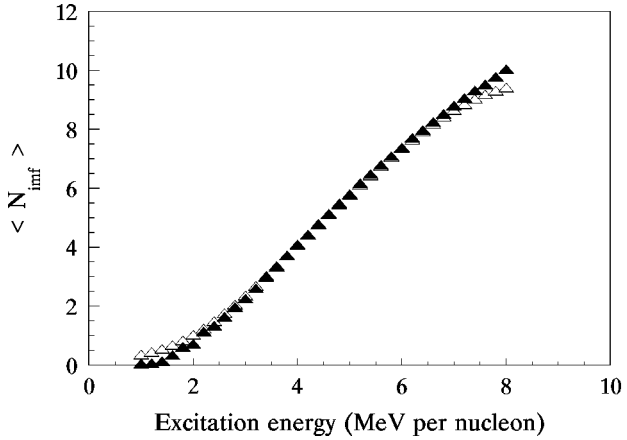

FIG. 1. Average IMF multiplicity calculated with the SMM as a function of the excitation energy of the nuclear system (solid triangles) and averaged over excitation energy (open triangles). See text for further details.

we do not consider secondary decay of the fragments, which would lower the curve shown in Fig. 1 and, eventually, lead to a saturation and decrease of the IMF multiplicity at high energies. As a matter of fact, the IMF multiplicity would even fall down to zero if one continued increasing the amount of excitation energy of the source; i.e., the system would tend to vaporize into single nucleons [36,37].

We now turn to the properties of the multifragment emission. The probability $P_n(E)$ of observing n fragments, for a source with excitation energy equal to E, is, following Refs. [29,31], given by

$$P_n(E)=\frac{N(E,n)}{\Sigma_n N(E,n)}, \tag{3.1}$$

where $N(E,n)$ stands for the number of events in which n IMF's are observed for an excitation energy per nucleon E.

The results are displayed in Fig. 2. It shows that very few IMF's are emitted by the source in the low excitation energy regime, $E\leqslant 2$ MeV per nucleon. Moreover, the maximum of $P_n(E)$ moves toward higher excitation energies. This behavior is in qualitative agreement with the experimental results reported in Refs. [29,31]. We have checked that these aspects remain unchanged if one considers larger emitting sources. However, as we will see in the next subsection, the characteristics of $P_n(E)$ predicted by the SMM are very different from those given by the molecular dynamics approach.

The experimental analysis reported in Refs. [29,31] provides stronger constraints on the functional form of $P_n(E)$. More specifically, it has been shown [29,31] that the probability of emitting n complex fragments follows a binomial law:

$$P_n^m=\frac{m!}{n!(m-n)!}p^n(1-p)^{m-n}. \tag{3.2}$$

The elementary binary probability p and the parameter m are determined from the observed IMF multiplicities by

$$\langle n\rangle = mp \tag{3.3}$$

and

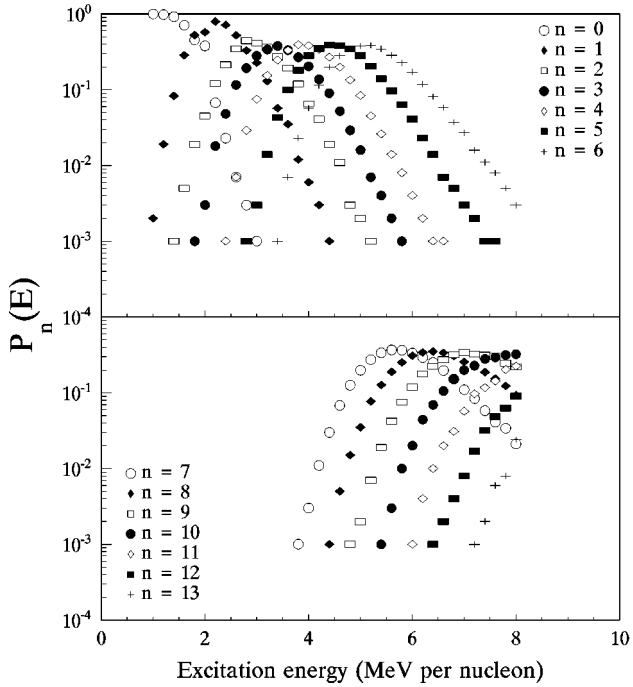

FIG. 2. Calculated probability of observing n IMF's as a function of the excitation energy of the source, for the same system of Fig. 1.

$$\sigma_n^2=\langle n\rangle(1-p), \tag{3.4}$$

where $\langle n\rangle$ is the average IMF multiplicity and σ_n^2 its variance for a given excitation energy E.

In order to investigate whether $P_n(E)$ obtained with the SMM has the properties of a binomial distribution, we have calculated the elementary binary probability p and the parameter m through Eqs. (3.3) and (3.4). The results of the model calculation are represented by the solid triangles in Fig. 3, while the experimental values for the ^{36}Ar (110 MeV per nucleon)+ ^{197}Au system, reported in Ref. [29], are depicted by the solid circles. One may notice that $1/p$ predicted by the SMM increases by $\approx$30% over the excitation energy range considered, while the experimental results increase by a much larger factor, of about 20. Furthermore, m increases almost linearly as a function of E, for $E>2$ MeV per nucleon, in contrast with the behavior observed in the experimental results.

The analysis in terms of the SMM is therefore compatible with a statistical decay of the source, but with different characteristics from those of Refs. [29,31]. According to this model, the binary decay probability p is almost constant and of the order of 1, while the number of tries m increases with excitation energy. The data seem to suggest that p increases considerably with the excitation energy while m remains approximately constant for not too low excitation energies.

The fact that the Arrhenius plot shown in the upper panel of Fig. 3 is rather flat compared to the behavior observed in Refs. [29,31] may be easily understood. The elementary binary probability shown in Fig. 3 is computed from the mean IMF multiplicities and variances predicted by the SMM using Eq. (3.4), which gives

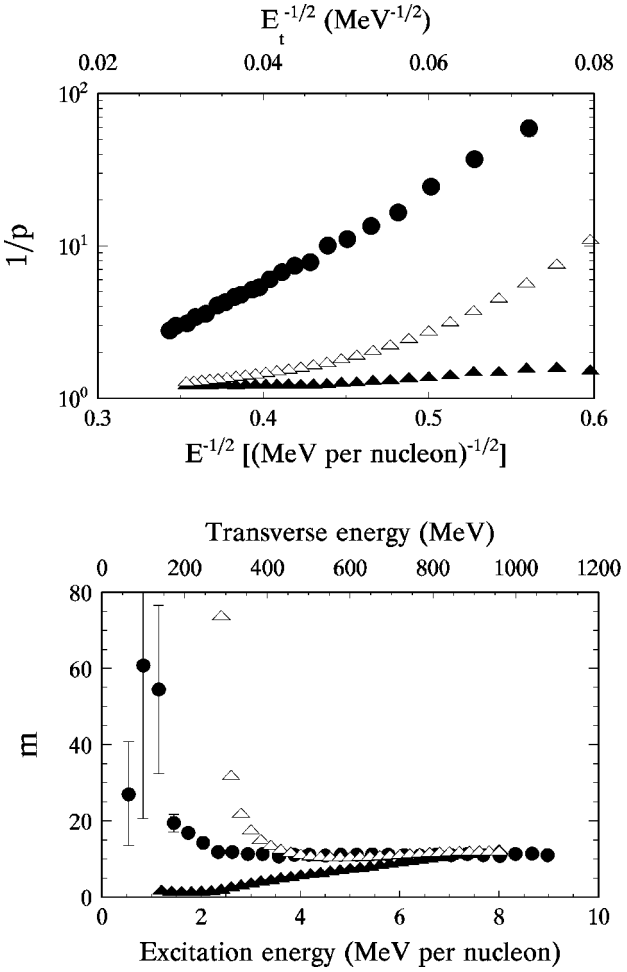

FIG. 3. Upper panel: reciprocal of the elementary binary probability deduced from SMM calculations as a function of the excitation energy E (solid triangles) and averaged over the excitation energy (open triangles), for the same system of Figs. 1 and 2. Also included are the values extracted from the $^{36}Ar+^{197}Au$ data, plotted as a function of the transverse energy E_t. Lower panel: same as the upper panel for the parameter m.

$$p = 1 - \frac{\sigma_n^2}{\langle n \rangle}. \tag{3.5}$$

Therefore $\sigma_n^2 \ll \langle n \rangle$, in the SMM calculations, while $\sigma_n^2 \approx \langle n \rangle$ in the data, except at the highest energies considered. Thus, the behavior of the Arrhenius plot presented here reveals that the variances of the IMF multiplicities predicted by the SMM are much smaller than those suggested from the data, at least at low excitation energies. We have checked that this conclusion still holds even if one changes the only parameter of the model, the breakup density, to, for example, $\rho = 0.03$ nucleons/fm^3. After the discussion on the MDM results, in the next subsection, we will find a likely explanation for this discrepancy.

B. Predictions of molecular dynamics

In order to study the properties of the probability distribution $P_n(E)$ of observing n IMF's emitted by a system whose initial excitation energy is E, we have run more than 40 000 events for the Xe (60 MeV per nucleon)+Au, system, also experimentally studied, using the molecular dynamics model described above. The impact parameters of the colliding nuclei were randomly chosen between 0 and 7 fm, with the appropriate weight so as to simulate as closely as possible the experimental situation. Since it is very difficult to reliably extract the excitation energy deposited into the system within the framework of this model, we have used the transverse energy E_t of charged fragments as a measure of the excitation energy of the system. This choice is based on studies recently reported in the literature which indicate that the transverse energy is proportional to the amount of energy deposited into the system (see [29,31] and references therein), where the coefficient of proportionality depends on the mass numbers of the colliding nuclei and on the bombarding energy.

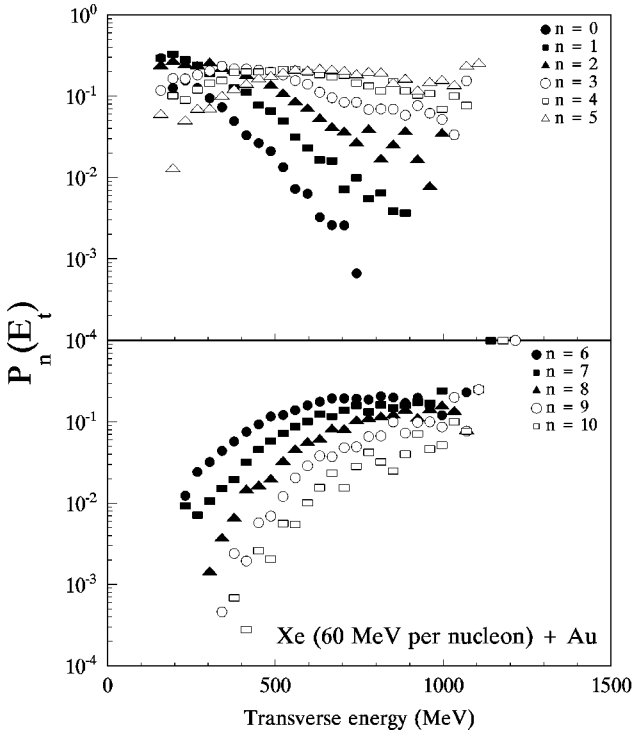

FIG. 4. Probability of observing n IMF's as a function of the fragments' transverse energy predicted by the molecular dynamics approach for the Xe+Au system.

The results of the model simulation are displayed in Fig. 4. It shows that the probability of observing n IMF's decreases monotonously as a function of E_t for n small ($n \leqslant 2$), whereas it is nearly flat for $3 \leqslant n \leqslant 5$. On the other hand, $P_n(E_t)$ increases very fast as a function of E_t for $n \geqslant 6$. These predictions might seem, at first sight, qualitatively similar to those of the SMM (Fig. 3). However, when an analysis in terms of the binary emission probability is performed, we note that they behave very differently.

Figure 5 displays the reciprocal of the elementary binary probability and the number of tries m, calculated through Eqs. (3.3) and (3.4), as a function of the transverse energy. The results obtained with the MDM are depicted by the open circles while the experimental data [31] are represented by the solid circles in the same figure. Comparison between the results of the MDM with the experimental data shows that this model is not able to reproduce, even qualitatively, the behavior found experimentally. As a matter of fact, although

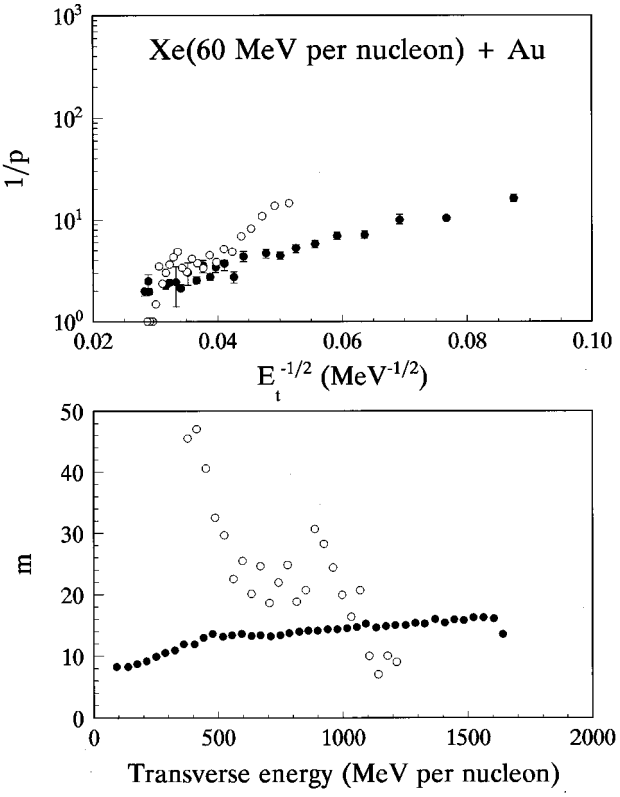

FIG. 5. Upper panel: reciprocal of the elementary binomial probability as a function of the transverse energy. Data values (solid circles), calculated with the MDM (open circles). Lower panel: same as the upper panel for the parameter m.

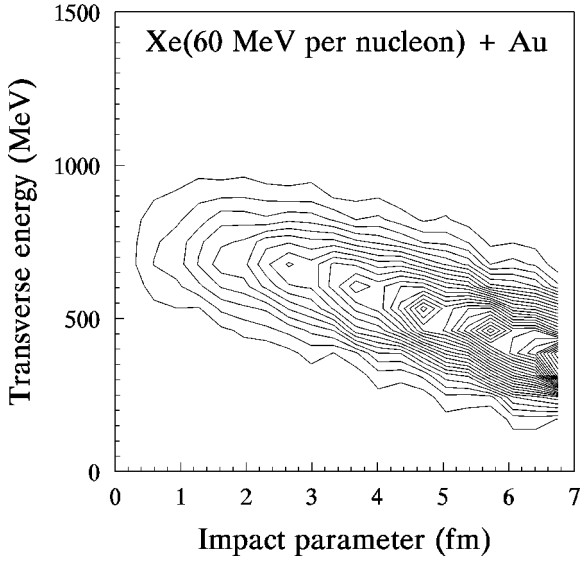

FIG. 6. Contour plot of the event distribution on the transverse-energy–impact-parameter plane.

the elementary binary probability predicted by this model increases as a function of the transverse energy, it assumes negative values for transverse energies smaller than ≈ 300 MeV. For this reason, we only show $1/p$ predicted by this model for transverse energies higher than this value. Furthermore, the number of tries, m, obtained with the MDM decreases as a function of the transverse energy, in clear conflict with the experimental observations. It thus appears that the MDM is not well suited to describe multifragment emission, at least at low excitation energies. In fact, as discussed in Refs. [35,38], the heat capacity of the molecular dynamics approach does not correspond to that of an actual many-fermion system, leading to fragmentation properties at variance with those experimentally observed. This is the reason why frequently the molecular dynamics description is stopped at an early point in the evolution of the collision, and another model, e.g., the SMM, is employed to describe the breakup.

At this point, it is useful to further discuss some features of the data. In Refs. [29,31], the properties of P_n have been analyzed by classifying events according to the transverse energy, and not on their centrality. Thus, it is important to verify the extent to which selection in transverse energy implies selection in impact parameter. Since the amount of energy transferred to the transverse motion should be mainly influenced by energy and momentum conservation, the molecular dynamics approach is able to give a good description of this aspect, at least semiquantitatively. The results of the model simulation are depicted by the contour plot in Fig. 6. It shows that the average value of the transverse energy increases as the impact parameter goes to zero. However, the dispersion around the mean value is very broad. In fact, our results show that events with a given transverse energy, e.g., 600 MeV, may originate from collisions which take place at almost any value of the impact parameter. The dynamics of collisions which occur in such a wide range of impact parameters should be very different, especially due to compression and angular momentum effects [39]. In particular, the partition of the transverse energy into components associated with thermal excitation and radial flow may change drastically with impact parameter.

The bunching under a similar label (e.g., transverse energy) of fragmentation events associated with very different processes could lead to a distorted picture. For instance, in discussing signals for a liquid-gas phase transition in nuclear matter, it was found that the power law dependence of inclusive fragment distributions was of geometrical origin [40]. In this context, this led the authors to the conclusion that it was important to single out experimental events associated with different impact parameters so as to allow one to discuss a possible liquid-gas phase transition in nuclear matter [40]. More closely related to the aspects we discuss here, it was shown in an independent work that the superposition of multifragmentation events associated with different excitation energies shows signs of intermittency, which are absent in events associated with a single excitation energy [41]. This behavior was explained in terms of the fragment multiplicity distribution. If narrow, as in the case of a single excitation energy, it shows no sign of intermittent behavior; if broad, as in the case where several excitation energies are pooled together, intermittency patterns emerge. In fact, we have noted that the rather constant behavior of the binary emission probability in the SMM arises from the narrowness of the fragment multiplicity distribution. This distribution is much wider in the data, which leads to a rapid change of this quantity. The situation appears to be similar as in the data showing intermittent behavior.

In order to make the assertions above more quantitative, let us consider the calculation of a physical quantity f, which

is a function of the excitation energy of the system. Owing to the large number of open decay channels for the system which passes through highly excited nonequilibrated sates, given the initial configuration of the decaying system (e.g., the impact parameter of the collision) its final excitation energy and, consequently, this quantity f vary from event to event. Thus, if one could strictly single out events with an actual excitation energy ϵ, f would be given by the average value of this quantity over all initial conditions which contribute to the excitation energy ϵ. We denote this average over events with excitation energy ϵ by $\langle f(\epsilon)\rangle$. However, it is not possible, in general, to define precisely the excitation energy of the system. Experimental events are selected according to criteria which mix, with weight $W(\epsilon-E)$, events with different excitation energies around their average value E. The measured value $f(E)$ is thus given by

$$f(E)=\frac{\int_{\epsilon_{\min}}^{\epsilon_{\max}} W(\epsilon-E)\langle f(\epsilon)\rangle d\epsilon}{\int_{\epsilon_{\min}}^{\epsilon_{\max}} W(\epsilon-E)d\epsilon}, \tag{3.6}$$

where E stands for the mean experimentally measured excitation energy, and $\epsilon_{\min}$ and $\epsilon_{\max}$ represent the minimum and maximum values of the excitation energy contributing to events with average excitation energy E, respectively.

In order to illustrate the effects of mixing events with different excitation energies on the analysis discussed in this work, we assume, for the sake of simplicity, that W is given by

$$W=\exp\left(-\frac{(\epsilon-E)^2}{2\sigma^2}\right), \tag{3.7}$$

where σ^2 is the variance of the distribution W. The results corresponding to consideration of this admixture in the ''pure'' events of the SMM are depicted by the open triangles in Figs. 1 and 3. The results shown in Fig. 1 reveal that the average IMF multiplicity is quite insensitive to the admixture. However, the reciprocal of the elementary binary probability p and the parameter m, represented by the open triangles in Fig. 3, deviates appreciably from the unfolded values. The results discussed here were obtained using $\sigma=0.7$ MeV in Eq. (3.7). There is no special reason for this particular choice, since we are only interested in illustrating the effects of the admixture of excitation energy on the analyses. We notice that the behavior of $1/p$ looks now very similar to that reported in Ref. [29] and shown in Fig. 3. It is also important to notice that the behavior of the parameter m is the same as the experimental one shown in this picture. This is due to the fact that, although the average value of the IMF multiplicity does not change appreciably, its variance is very sensitive to the admixture of excitation energies. Therefore, our analysis strongly suggests that the discrepancies between the SMM and the experimental data are essentially due to the fact that different excitation energy values are mixed in the data analyses. As already mentioned, the measured transverse energies have contributions from thermal, rotational, and radial flow energies, in contrast with the model calculation in which only the thermal component is considered.

IV. SUMMARY AND CONCLUDING REMARKS

We have investigated the properties of the multifragment emission predicted by two models based on completely different scenarios for the nuclear multifragmentation process: a statistical multifragmentation model in which one assumes a simultaneous breakup of the source and a molecular dynamics approach where dynamic instabilities lead to the dissociation of the system. The latter turned out to be unable to reproduce, even qualitatively, the binomial properties of the probability of n-fragment emission observed experimentally. This apparent failure of a dynamical model does not imply that dynamical effects do not affect the fragmentation process. This shortcoming may be understood in terms of the inherent deficiencies of the MDM, such as its classical heat capacity, which prevent it from successfully describing some aspects of the nuclear multifragmentation phenomenon. It will be important to ascertain whether a more sophisticated model such as the so-called fermionic molecular dynamics [42] leads to a correct description of the data. Unfortunately, this model has only been applied to considerably lighter systems [43] than those studied by Moretto *et al.*

The SMM has proved to be able to describe the qualitative features observed in the multifragment emission. However, in the process of understanding the description through this statistical model, we have shown that the data may be grouping together processes with the same transverse energy but associated with different impact parameters, which correspond to different excitation mechanisms. It would be important to repeat the data analysis trying to disentangle, e.g., through the momentum flow tensor, the peripheral from the more central collision events so as to introduce a more strict filter on the excitation energy of the source.

ACKNOWLEDGMENTS

We are very grateful to Dr. L. G. Moretto for stimulating discussions. We would like to thank partial financial support from the Conselho Nacional de Pesquisas (CNPq) and the Fundação à Pesquisa do Estado do Rio de Janeiro (FAPERJ).

[1] D. Q. Lamb, J. M. Lattimer, C. J. Pethick, and D. G. Ravenhall, Phys. Rev. Lett. **41**, 1623 (1978).

[2] H. R. Jaqaman, A. Z. Mekjian, and L. Zamick, Phys. Rev. C **27**, 2782 (1983); **29**, 2067 (1984).

[3] P. J. Siemens, Nature (London) **305**, 410 (1983); G. Bertsch and P. J. Siemens, Phys. Lett. **126B**, 9 (1983).

[4] M. W. Curtin, H. Toki, and D. L. Scott, Phys. Lett. **123B**, 289 (1983).

[5] A. D. Panagiotou, M. W. Curtin, H. Toki, D. K. Scott, and P. J. Siemens, Phys. Rev. Lett. **52**, 496 (1984).

[6] J. Kapusta, Phys. Rev. C **29**, 1735 (1984).
[7] A. L. Goodman, J. Kapusta, and A. Z. Mekjian, Phys. Rev. C **30**, 851 (1984).
[8] D. H. Boal and A. L. Goodman, Phys. Rev. C **33**, 1690 (1986).
[9] B. Jakobsson, G. Jönson, L. Karisson, B. Lindkvist, and A. Oskarsson, Z. Phys. A **307**, 293 (1982).
[10] J. E. Finn *et al.*, Phys. Rev. Lett. **49**, 1321 (1982).
[11] R. W. Minich *et al.*, Phys. Lett. **118B**, 458 (1982).
[12] C. B. Chitwood, C. K. Gelbke, W. G. Lynch, A. D. Panagiotou, M. B. Tsang, H. Utsunomiya, and W. A. Friendman, Phys. Lett. **131B**, 289 (1983).
[13] E. M. Friedlander, H. H. Heckman, and Y. J. Karant, Phys. Rev. C **27**, 2436 (1983).
[14] A. I. Warwick *et al.*, Phys. Rev. C **27**, 1083 (1983).
[15] A. S. Hirsch, A. Bujak, J. E. Finn, L. J. Gutay, R. M. Minich, N. T. Porile, R. Scharenberg, B. C. Stringfellow, and F. Turkot, Phys. Rev. C **29**, 508 (1984); C. J. Waddington and P. S. Freier, *ibid.* **31**, 888 (1985); A. Bujak, J. E. Finn, L. J. Gutay, A. S. Hirsch, R. W. Minich, G. Paderewski, N. T. Porile, R. P. Scharenberg, B. C. Stringfellow, and F. Turkot, *ibid.* **32**, 620 (1985).
[16] J. Randrup and S. E. Koonin, Nucl. Phys. **A356**, 223 (1981).
[17] W. A. Friedman and W. G. Lynch, Phys. Rev. C **28**, 26 (1983).
[18] J. Aichelin, J. Hüfner, and R. Ibarra, Phys. Rev. C **30**, 107 (1984); J. Aichelin and J. Hüfner, Phys. Lett. **136B**, 15 (1984).
[19] W. Bauer, D. R. Dean, U. Mosel, and U. Post, Phys. Lett. **150B**, 53 (1984); T. S. Biro, J. Knoll, and J. Richert, Nucl. Phys. **A459**, 692 (1986); X. Campi, J. Phys. A **19**, L917 (1986); Phys. Lett. B **208**, 351 (1988); C. Ngô, H. Ngô, S. Leray, and M. Spina, Nucl. Phys. **A337**, 148 (1989).
[20] D. H. E. Gross, L. Satpathy, T. C. Meng, and M. Satpathy, Z. Phys. A **309**, 41 (1982).
[21] J. P. Bondorf, R. Donangelo, I. N. Mishustin, C. J. Pethick, H. Schulz, and K. Sneppen, Nucl. Phys. **A443**, 321 (1985); J. P. Bondorf, R. Donangelo, I. N. Mishustin, and H. Schulz, *ibid.* **A444**, 460 (1985); H. W. Barz, J. P. Bondorf, R. Donangelo, I. N. Mishustin, and H. Schulz, *ibid.* **A448**, 753 (1985).
[22] D. H. E. Gross, Rep. Prog. Phys. **53**, 605 (1990).
[23] J. P. Bondorf, A. S. Botvina, A. S. Iljinov, I. N. Mishustin, and K. Sneppen, Phys. Rep. **257**, 133 (1995).
[24] G.F. Bertsch and S. Das Gupta, Phys. Rep. **160**, 189 (1988); P. Schuck, R. W. Hasse, J. Jaenicke, C. Grégoire, B. Remaud, F. Sebille, and E. Suraud, Prog. Part. Nucl. Phys. **22**, 181 (1989); A. Bonasera, F. Gulminelli, and J. Molitoris, Phys. Rep. **243**, 1 (1994).
[25] J. Aichelin, Phys. Rep. **202**, 233 (1991).
[26] L. G. Moretto and G. J. Wozniak, Annu. Rev. Nucl. Part. Sci. **43**, 379 (1993).
[27] J. Pochodzalla *et al.*, Phys. Rev. Lett. **75**, 1040 (1995).
[28] L. G. Moretto, D. N. Delis, and G. J. Wozniak, Phys. Rev. Lett. **71**, 3935 (1993).
[29] L. G. Moretto *et al.*, Phys. Rev. Lett. **74**, 1530 (1995).
[30] L. G. Moretto, K. X. Jing, and G. J. Wozniak, Phys. Rev. Lett. **74**, 3557 (1995); L. Phair *et al.*, *ibid.* **75**, 213 (1995).
[31] K. Tso *et al.*, Phys. Lett. B **361**, 25 (1995).
[32] S. R. Souza, L. S. de Paula, S. Leray, J. Nemeth, C. Ngô, and H. Ngô, Nucl. Phys. **A571**, 159 (1994).
[33] K. Sneppen, Nucl. Phys. **A470**, 213 (1987).
[34] J. P. Bondorf, A. S. Botvina, I. N. Mishustin, and S. R. Souza, Phys. Rev. Lett. **73**, 628 (1994).
[35] R. Donangelo and S. R. Souza, Phys. Rev. C **52**, 326 (1995).
[36] C. A. Ogilvie *et al.*, Phys. Rev. Lett. **67**, 1214 (1991).
[37] G. F. Peaslee *et al.*, Phys. Rev. C **49**, 2271 (1994).
[38] R. Donangelo, H. Schulz, K. Sneppen, and S. R. Souza, Phys. Rev. C **50**, R563 (1994).
[39] L. De Paula, J. Nemeth, Ben-Hao Sa, S. Leray, C. Ngô, H. Ngô, S. R. Souza, and Yu-Ming Zheng, Phys. Lett. B **258**, 251 (1991).
[40] G. Peilert, H. Stöcker, W. Greiner, A. Rosenhauer, A. Bohnet, and J. Aichelin, Phys. Rev. C **39**, 1402 (1989).
[41] H. W. Barz, J. P. Bondorf, R. Donangelo, I. N. Mishustin, H. Schulz, and K. Sneppen, Phys. Rev. C **45**, 2541 (1992).
[42] H. Feldmeier, Nucl. Phys. **A515**, 147 (1990).
[43] H. Feldmeier and J. Schnack, in *Proceedings of the XXII International Workshop on Gross Properties of Nuclei and Nuclear Excitations*, Hirschegg, 1994, edited by H. Feldmeier and W. Nöremberg (GSI, Darmstadt, 1994), p. 207.